Deuteron NMR investigation of a photomechanical effect in a smectic-*A* liquid crystal

Boštjan Zalar
Jožef Stefan Institute, University of Ljubljana, Jamova 39, 1000 Ljubljana, Slovenia

Oleg D. Lavrentovich
Chemical Physics Interdisciplinary Program and Liquid Crystal Institute, Kent State University, Kent, Ohio 44242-0001

Huairen Zeng* and Daniele Finotello
Department of Physics, Kent State University, Kent, Ohio 44242-0001
(Received 22 February 2000)

Deuteron quadrupole-perturbed NMR is used to study the perturbation of orientational order in a smectic-*A* liquid crystal (octylcyanobiphenyl or 8CB) caused by photoinduced *trans*-to-*cis* isomerization of a photosensitive dopant (diheptylazobenzene or 7AB). The time and temperature dependences of the orientational order were independently studied for 8CB, 7AB, and their mixtures. Upon UV irradiation that causes *trans*-to-*cis* isomerization of 7AB, the orientational order parameter of the smectic-*A* phase is reduced. Relaxation in the dark exponentially restores the equilibrium value of the order parameter. The characteristic time for this process closely matches the lifetimes of the 7AB excited state. While in the 8CB smectic-*A* matrix, the *cis*-isomerized 7AB molecules retain a uniaxial orientational order with the director oriented along the normal to the smectic layers. The highly bent 7AB *cis* molecules act as a disorienting factor, decreasing the orientational order in the layers and causing a small increase in layer spacing. This disorder-induced increase in layer spacing is much smaller than the actual increase as observed by *in situ* x-ray experiments on UV-irradiated mixtures of 8CB:7AB. Concomitant with the experimental observation that only a fraction of 7AB molecules are converted to the *cis* state, this work provides indirect evidence for a nanophase segregation with the 7AB *cis*-isomers arranged within the interlayer space, thus significantly increasing the smectic layer spacing.

PACS number(s): 61.30.Gd, 64.70.Md, 76.60.−k

I. INTRODUCTION

Optical control of the molecular order in liquid crystal (LC) phases has attracted considerable attention as an interesting phenomenon caused by a number of different mechanisms, some of which, as discussed in recent reviews [1–5], are not well understood. The interest is stimulated by the fact that achieving alignment control by optical means offers potential applications in display and optoelectronic devices [1]. Particularly effective means to cause a photosensitive response are through photoisomerization (e.g., *trans*-to-*cis* or *cis*-to-*trans*) of the liquid crystal molecules or through foreign molecules either added to the liquid crystal bulk or forming a surface alignment layer.

Although most studies to date have dealt with the nematic phase [1–5], recently, a number of photochemical effects have also been reported for the smectic phases of thermotropic [6–10] as well as lyotropic [11] liquid crystal materials. In smectic phases, photochemical effects influence not only the orientational, but also the positional order; consequently, they give rise to photomechanical phenomena such as changes in the layer spacing and subsequent undulations of layers or the formation of focal conic domains [12,13]. *In situ* x-ray studies [14] have shown that when the smectic-*A* (Sm-*A*) mixture of octylcyanobiphenyl (8CB) and photosensitive diheptylazobenzene (7AB) is irradiated with short-wavelength (UV) light that enriches the system with *cis*-isomers of 7AB, the layer thickness increases by about 0.5%. The subsequent shrinkage to the equilibrium thickness can be significantly accelerated by irradiation at a longer wavelength (such as 633 nm, He-Ne laser) that facilitates *cis*-to-*trans* isomerization. The effect of layer shrinkage under He-Ne irradiation suggests that the prime mechanism responsible for the photocontrol of smectic layer spacing is photochemical rather than thermal through the heating of the sample (the layer spacing of the 8CB:7AB mixture increases with temperature [14]). There is also further indirect evidence of a photochemical mechanism in that the characteristic times of the layers contractions are quite similar to the lifetime of *cis*-isomers of azodye molecules [15].

The molecular rearrangements of the Sm-*A* phase responsible for the photocontrol of layer spacing remain to be studied. Recent computer simulations [16] predict photoinduced nanophase segregation: strongly bent 7AB *cis*-isomers cannot accommodate themselves within the layers and thus migrate to locations between the layers, consequently accounting for an increase in layer thickness. Upon relaxation, rodlike *trans*-isomers return to within the layers and the layer thickness decreases. Nanophase segregation is also supported by the prediction [17] that even in pure smectic systems composed of identical rodlike molecules, a small fraction of them could be located in the space between the smectic layers, aligned transversely to the rest of the molecules. However, the photoinduced changes can also be explained by a somewhat simpler mechanism based on the idea that the *cis*-isomers decrease the orientational order parameter of the

*Present address: Yale School of Medicine, P.O. Box 208042-Fitkin B, New Haven, CT 06520.

smectic phase. This, in turn, increases the smectic layer spacing through the coupling between orientational and positional ordering, in a manner similar to the increase of layer spacing with increasing temperature. Therefore, in this work, in order to shed additional light onto the microscopic origin of the photocontrol of smectic spacing, we employ deuteron quadrupole-perturbed NMR (DNMR) spectroscopy which is extremely sensitive to changes in the orientational order of liquid crystal molecules to study the behavior of 8CB:7AB mixtures.

This paper is organized as follows. In Sec. II, we describe the system under study and detail the methods of sample preparation. After reviewing some of the technical aspects of the DNMR technique in Sec. III, we present and discuss the DNMR experimental results in Sec. IV. Concluding remarks can be found in Sec. V.

II. MATERIALS

Diheptylazobenzene is a mesogenic material that forms a nematic phase and a monotropic (during cooling) smectic-*A* phase [18,19]. Although its photosensitivity was apparently not an issue of concern in earlier studies, it can be easily verified by a simple polarizing-microscope experiment. Under regular ''white'' illumination, 7AB shows an enantiotropic nematic phase, about 7 K wide, with the melting point at 313.2 K and the clearing [nematic-isotropic (NI)] transition at 320.2 K [18]. If the sample is irradiated with UV light, the phase width shrinks, eventually disappearing; the material is in the isotropic state even at room temperature. The reason for this is the UV-provoked *trans*-to-*cis* isomerization of 7AB [13]. Isomerization of 7AB is similar to that of azobenzene and its other derivatives, and shows a dramatic steric effect: the *trans*-isomers have a rodlike elongated structure, approximately 29 Å long, while the *cis*-isomers are highly bent (U shaped) with a characteristic size of about 16 Å, seen in Fig. 1.

The stationary fraction c of the *cis*-isomers present in the system changes widely between 0 and 1 (never reaching the limits) depending on the wavelength of the irradiating light [20]. A high population of *cis*-isomers is typically achieved under UV irradiation: for azobenzene solutions in isooctane, $c=0.8$ at $\lambda=313\,\mathrm{nm}$ [19]. The conversion into the ground *trans* state occurs either through thermal relaxation in the dark or under light irradiation at longer wavelengths (typically >420 nm). For example, for the azobenzene solutions mentioned earlier c decreases to 0.045 at $\lambda=578\,\mathrm{nm}$ [19].

The liquid crystal host matrix used in this work was octylcyanobiphenyl (8CB) with the phase transition sequence

$$\mathrm{I} \xrightarrow{313.5\ \mathrm{K}} \mathrm{N} \xrightarrow{306.5\ \mathrm{K}} \mathrm{Sm}\text{-}A \xrightarrow{294.5\ \mathrm{K}} \mathrm{Cr}.$$

In the smectic-*A* phase, 8CB molecules form dimers and the layer thickness varies between 31.4 and 31.6 Å as the temperature increases [14]. Thus the length of 7AB *trans*-isomers matches well the 8CB layer thickness. As a result, a small amount of 7AB solute (up to 16% by weight) does not change significantly the phase diagram of pure 8CB [12].

To ensure DNMR sensitivity to 7AB and 8CB, selectively deuterated analogs of both compounds were prepared. The two protons at the α position (or first position) of the respective aliphatic chains were replaced by deuterons. Each 8CB(D) molecule contained only a pair of deuterons since there is only one $C_8H_{15}D_2$ alkyl chain attached to the molecular core. In contrast, the 7AB(D) molecules contained four deuterons each, since there are two $C_7H_{13}D_2$ chains attached to the molecular core at opposite sides.

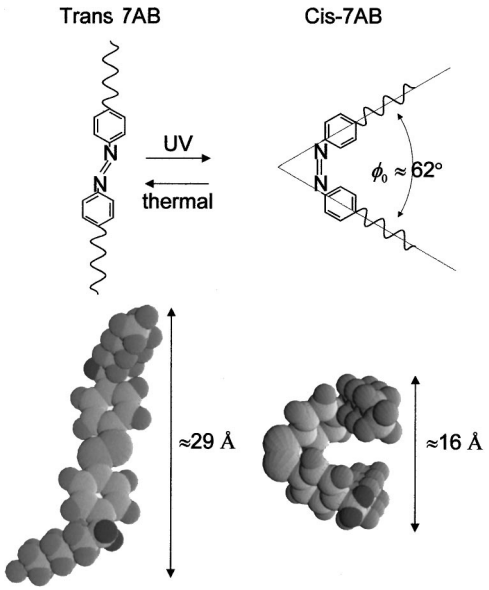

FIG. 1. Schematic representation of the 7AB isomerization process (top) and a three-dimensional view of the two isomeric states (bottom). The two flexible alkyl chains attached to the two phenyl rings of the rigid molecular core on opposite sides are shown in one of the many possible conformations. Deuterated sites are drawn with a darker gray level.

Four different samples were investigated in this study: pure 8CB(D), pure 7AB(D), a mixture of 8CB:7AB(D), and a mixture of 8CB(D):7AB. The pure 8CB(D) (nonphotosensitive) served as a base reference of the orientational ordering. The 7AB(D) NMR spectrum was measured in order to properly identify spectral absorption peaks as pertaining to *trans* and *cis* isomers. The two mixtures 8CB:7AB(D) and 8CB(D):7AB, of complementary deuteration, were prepared to separate the 8CB spectral absorption peaks from those of 7AB. Specifically, the 8CB:7AB(D) mixture served to study the orientational order of 7AB in the 8CB host. The 8CB(D):7AB mixture, on the other hand, was investigated to determine possible changes in the 8CB orientational order that might be caused by (a) the very presence of the 7AB dye molecules and by (b) changes in the fraction of 7AB *cis*-isomers. Both mixtures were prepared with the same 8CB:7AB weight ratio of 90.67:9.33, which closely matches the concentration used in the x-ray measurements of smectic layer spacing [14,21]. The mixture chosen resulted in the following 8CB:7AB(D) and 8CB(D):7AB phase sequence:

$$\mathrm{I} \xrightarrow{317.6\ \mathrm{K}} \mathrm{N} \xrightarrow{311\ \mathrm{K}} \mathrm{Sm}\text{-}A \xrightarrow{<275\ \mathrm{K}} \mathrm{Cr}.$$

The samples for DNMR studies were prepared by sealing the corresponding bulk samples into thin-wall, UV-transparent, cylindrically shaped glass sample holders of 5 mm diameter and 25 mm length.

III. EXPERIMENTAL DETAIL

A. Deuteron NMR

The usefulness of deuteron NMR (DNMR) in the study of the molecular orientational behavior in liquid crystals has been demonstrated in numerous studies [22,23]. Most of these studies dealt with rodlike molecules deuterated in the α position of the alkyl chain. In the bulk uniaxial nematic phase, fast reorientations of such molecules around the long molecular axis, as well as fast internal exchange of the two deuterons in the CD_2 group, yield a cylindrically symmetric electric field gradient (EFG) tensor at the deuteron site, with the symmetry axis pointing approximately along the long molecular axis. Previous DNMR studies [24] of *trans*-7AB have indeed shown that both the orientational order of aromatic rings and the rotations of the CD_2 group about the phenyl-C bond possess axial symmetry. This makes the two CD_2 deuteron sites indistinguishable, producing a DNMR spectrum consisting of two satellite absorption lines forming a doublet with quadrupole-perturbed frequency splitting:

$$\Delta\nu_{trans}(\theta)=\frac{3}{2}\nu_Q S_{trans}P_2(\cos\theta)$$

$$=\frac{3}{4}\nu_Q S_{trans}[3\cos^2\theta-1]. \qquad (1)$$

Here ν_Q is the time-averaged quadrupole coupling constant with magnitude $\approx$60 kHz at the α position [25,26], S_{trans} is the nematic scalar order parameter, and θ is the angle between the time-averaged orientation of the molecular long axis (i.e., the nematic director) and the external magnetic field. Equation (1) can be used to describe 8CB and *trans*-7AB liquid crystals since in both cases their molecules have elongated shapes. This is, however, not true for *cis*-7AB as *cis*-isomers are highly bent. The angle ϕ_0 between the two heptylazobenzene rodlike molecular fragments, connected by the N=N bond, is approximately $\approx$62° (see Fig. 1). These ''boomerang''-shaped molecules are expected to perform some general type of reorientational motions as a function of time. If these reorientations are very fast on the DNMR time scale $\tau_{\mathrm{NMR}}\approx(\nu_Q^{trans})^{-1}$ and possess cylindrical symmetry so that the uniaxial character of the nematic and smectic phases is retained, they would yield a decreased value of the nematic order parameter.

To describe the 7AB molecules, we shall adopt a simplified picture where (1) reorientational motion takes place about one or two perpendicular, independent axes that are fixed in the liquid crystal reference frame; (2) the reorientations are symmetric—the two elongated fragments of the 7AB molecule exhibit, on the time average, exactly the same reorientational motions; and (3) the 7AB molecules are rigid, and thus no conformational changes occur during reorientations. Note that to satisfy the above conditions, if only one reorientational axis existed, such an axis would be the axis of uniaxial symmetry. It is well known that for an EFG tensor of cylindrical symmetry of largest eigenvalue V_{zz} and corresponding eigenvector $\vec{z}$ performing stochastic reorientations on the surface of a cone, the time-averaged EFG tensor has a cylindrical symmetry around the symmetry axis $\vec{z}'$ of this cone. The largest eigenvalue reduces to $V_{z'z'}$

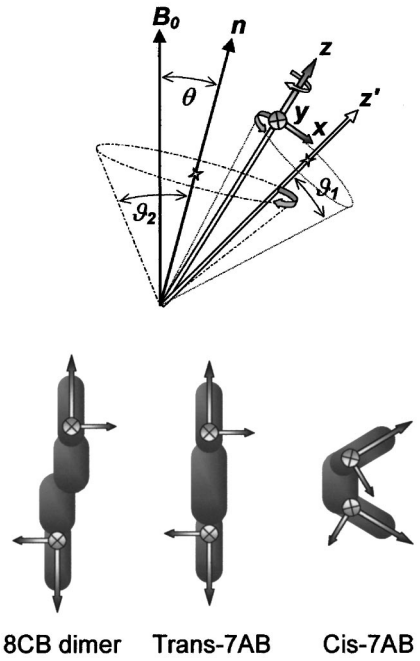

FIG. 2. Rotational motions (top), resulting in a partial averaging of the deuteron EFG tensor. The *x*-*y*-*z* frame is fixed to the first carbon atom of alkyl chain, with *z* pointing along the carbon-carbon bond joining the phenyl ring and the alkyl chains. Bottom: the position with respect to the three different molecular types forming the 8CB:7AB layers is shown. In contrast to 8CB dimers and *trans*-7AB, the two alkyl chains can be, in general, physically nonequivalent in *cis*-7AB, since the *z* directions of the two respective frames are not parallel. The selection of *x* and *y* axes is arbitrary due to fast reorientations around *z*. Here *z* and z' are ''free'' axes and *n* is the direction of the normal to smectic layers, while θ denotes the sample orientation with respect to the external magnetic field B_0. Also, ϑ_1 and ϑ_2 (see text) are the angular cone parameters.

$=P_2(\cos\vartheta_1)V_{zz}$, with ϑ_1 denoting the constant angle between $\vec{z}$ and $\vec{z}'$. The second reorientational process can be regarded as a stochastic precession of the cone axis $\vec{z}'$ around the director $\hat{n}$, i.e., about the axis of local cylindrical symmetry (see Fig. 2), decreasing the largest eigenvalue to $V_{nn}=P_2(\cos\vartheta_2)V_{z'z'}$, with ϑ_2 the angle between $\vec{z}'$ and $\hat{n}$. Given the proportionalities $\Delta\nu_{trans}\propto V_{zz}$ and $\Delta\nu_{cis}\propto V_{nn}$, the relation between *cis* and *trans* DNMR doublet splittings can be written as

$$\Delta\nu_{cis}(\theta)=\Delta\nu_{trans}(\theta)P_2(\cos\vartheta_1)P_2(\cos\vartheta_2). \qquad (2)$$

The nematic order parameter is a second-rank tensor [27]: thus, its components obey the same transformation rules as the components of the EFG tensor. Accordingly, the scalar part S_{cis} of the *cis*-7AB nematic order parameter is

$$S_{cis}=S_{trans}P_2(\cos\vartheta_1)P_2(\cos\vartheta_2), \qquad (3)$$

and Eq. (2) becomes

$$\Delta\nu_{cis}(\theta)=\Delta\nu_{trans}(\theta)\frac{S_{cis}}{S_{trans}}. \qquad (4)$$

The *trans*-to-*cis* isomerization of the 7AB molecules should be reflected in the DNMR spectrum through a de-

crease in the frequency splitting. This is a consequence of $|P_2(\cos\vartheta_1)P_2(\cos\vartheta_1)|\leqslant 1$, which implies that $S_{cis}\leqslant S_{trans}$. Thus measurements of the quadrupole frequency splitting as a function of sample orientation in the external magnetic field verify the local symmetry. When the local uniaxial symmetry of 7AB molecules is retained during a *trans*-to-*cis* isomerization, both $\Delta\nu_{trans}(\theta)$ and $\Delta\nu_{cis}(\theta)$ must follow the $P_2(\cos\theta)$ angular dependence.

B. Spectrometer and temperature control

DNMR measurements were performed in a 4.7-T superconducting magnet at the deuteron Larmor frequency of $\nu_L(^2\mathrm{H}) = 30.8\,\mathrm{MHz}$. DNMR spectra were obtained by a complex Fourier transform of the solid-echo time domain response to a $90°_x$-τ-$90°$-τ pulse sequence with phase cycling, 90° pulse length of 3 μs, $\tau = 80$ μs, and a repetition time of 200 ms. The signal was typically accumulated 5000 times. The temperature of the sample was controlled by an oven housed in the magnet bore, providing temperature stability better than 0.025 K over the temperature range of the measurements.

C. Samples preparation

To simplify the discussion, we will label the state with the minimum possible amount of *cis*-isomers as the *trans* state. Such a *trans* state was obtained by maintaining the samples in the dark in the NMR probe head, which was inserted in the magnet at a temperature $T = 323.2\,\mathrm{K}$ for 6 h. At this temperature, all the materials of interest, 8CB(D), 7AB(D), 8CB:7AB(D), and 8CB(D):7AB, are in the isotropic fluid phase. Light conditions facilitated the conversion of the 7AB molecules to the ground *trans* state.

Cis-isomerization was achieved by UV illumination of the sample. Since the NMR probe-head design does not allow for *in situ* illumination, an external temperature-controlled water bath with UV-transparent glass walls was used. The *trans* (non-UV-illuminated) sample was thermally stabilized and field aligned by keeping it for 1 h in the NMR magnet at the desired temperature. Simultaneously, the temperature of the external bath was set to the same value as that of the NMR cryostat. The sample was then removed from the magnet and placed in the external water bath. This was done as rapidly as possible (within 3 s), in order to maintain the sample temperature constant. Then, a UV-light beam of intensity $j \approx 1\,\mathrm{W/cm^2}$ was shone from the outside onto the sample and the illumination maintained for 2–4 h. During this period, the temperature increase of the water bath due to the illumination was compensated for by the addition of colder water; the empty NMR probe head was left in the magnet at the same temperature. Finally, the sample was rapidly reinserted into the NMR probe and in the magnet and the measurement started. Particular attention was given to smectic samples to ensure that the probe was inserted in the magnet in such a way that the sample had the same orientation as before the illumination. A different orientation placement of the sample would destroy the layer structure since the magnetic field tends to orient the layers normal parallel to its direction. In the nematic phase, this is not critical since all molecular directors are quickly realigned along the magnetic field within a fraction of a second [28].

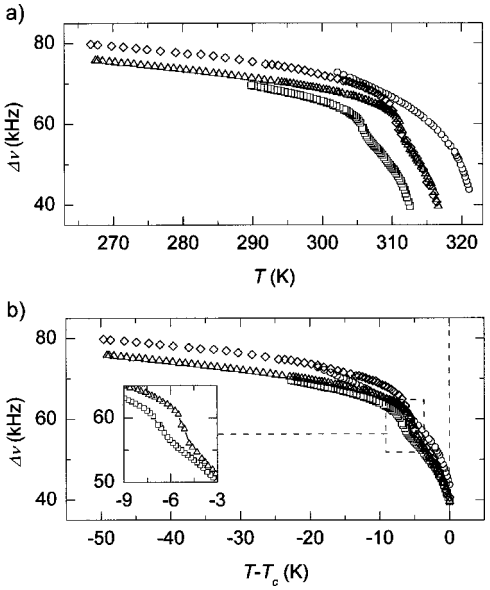

FIG. 3. (a) Temperature and (b) relative temperature dependences of the DNMR doublet frequency splitting of 8CB(D) and 7AB(D) (squares and circles, respectively) and for the 8CB(D):7AB (triangles) and 8CB:7AB(D) (diamonds). The inset is a magnified view near the nematic to smectic-*A* transition showing only 8CB(D) and 8CB(D):7AB data for clarity reasons.

IV. RESULTS AND DISCUSSION

A. Orientational order in *trans*-isomerized 7AB and 8CB:7AB mixtures

The nematic order parameter for a system of rodlike molecules can be determined from the DNMR quadrupole frequency splitting using Eq. (1). The splitting was measured in bulk ''*trans*'' (or non-UV-irradiated) 7AB(D), 8CB:7AB(D), 8CB(D):7AB, and 8CB(D). The results of these studies are presented in Fig. 3(a) at an orientation $\theta = 0°$ (parallel to the external field) for which $\Delta\nu(T) = \frac{3}{2}S\nu_Q$. In all four systems, only one pair of satellite absorption peaks with a frequency splitting $\Delta\nu(T)$ was observed. The chemical neighborhoods of the α-deuterons in 8CB(D) and 7AB(D) molecules are almost identical, so the value of $\nu_Q \approx 60\,\mathrm{kHz}$ found in 8CB(D) presumably matches that in *trans*-7AB(D). The relative difference in quadrupole frequency splitting between 8CB(D) and 7AB(D) thus measures the relative differences in order *S*.

The nematic to isotropic transition temperature $T_{\mathrm{N1}} = 317.6\,\mathrm{K}$ is the same in 8CB:7AB(D) and 8CB(D):7AB. The quantitative similarity of the respective frequency splittings in the nematic phase directly demonstrates that the nematic order parameters are close for 8CB(D) and *trans*-7AB(D). With decreasing temperature and approaching the smectic phase, the ''anomaly'' in $\Delta\nu(T)$, namely, a sudden enhancement in orientational order, is more pronounced for 8CB(D):7AB where an increase of about 6 kHz/K compared to 4 kHz/K for pure 8CB(D) occurs; see the inset to Fig. 3(b). This suggests that the nematic-smectic order parameter coupling is slightly stronger in the mixture including 7AB molecules than in pure 8CB even though the width of the nematic range is basically the same in both samples. Over the temperature range studied, the relative difference in fre-

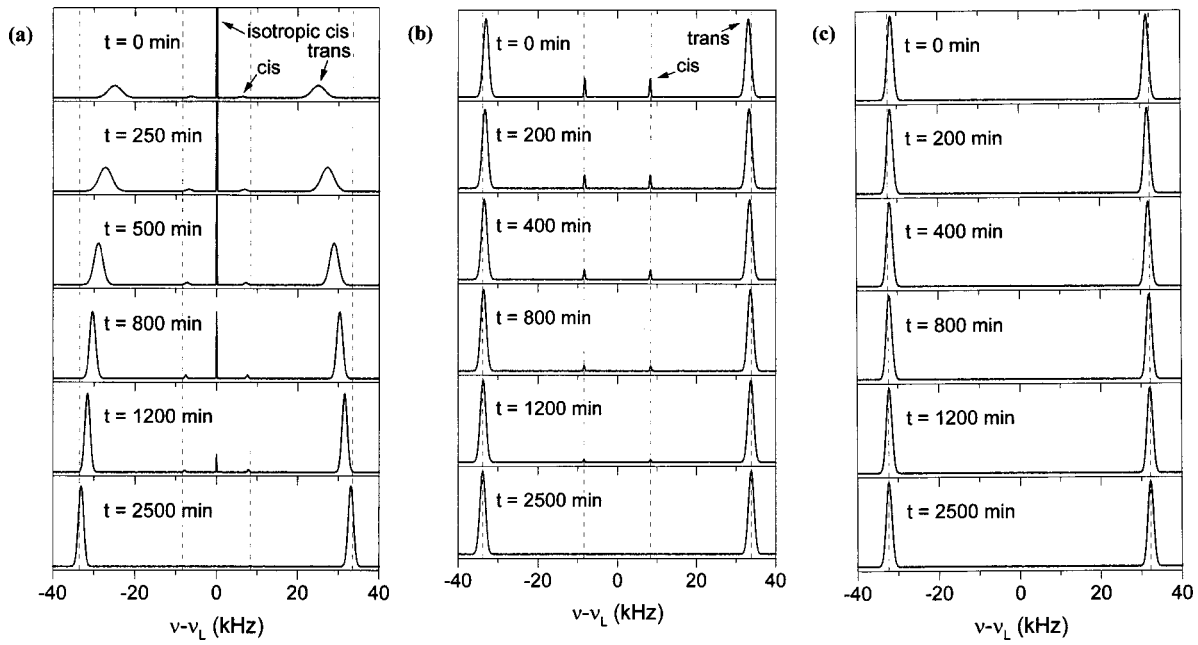

FIG. 4. Time dependence of the (a) 7AB(D), (b) 8CB:7AB(D), and (c) 8CB(D):7AB DNMR spectra observed after removal of UV illumination. The respective temperatures are $T=308.6$ K for (a) and (c) and $T=308.2$ K for (b).

quency splitting (S) between these samples remains at 8% or less.

Considering the critical behavior and differences in transition temperatures, a proper comparison of the orientational order of the mixed systems and the two pure compounds is obtained from inspecting the $\Delta\nu$ vs $T-T_c$ plot shown in Fig. 3(b), with T_c representing the respective transition temperatures into the isotropic phase. The general observation is that since $\Delta\nu(T)$ of 7AB(D) and 8CB(D) molecules in the mixed compound always exceeds $\Delta\nu(T)$ of pure 8CB(D), the presence of *trans*-7AB in the 8CB host increases S. This is expected since 8CB molecules are considerably shorter than the 7AB ones, and the 8CB smectic layers consist of dimers that are more flexible than the 7AB molecules (see Fig. 1). Similar arguments can be used to understand why the frequency splitting of bulk 7AB(D) is always greater than that of bulk 8CB(D).

B. Relation between orientational order and population of *cis*-isomerized 7AB

To elucidate how the orientational order for the 8CB:7AB mixtures is affected by the presence of *cis*-7AB isomers, UV-illuminated samples were probed; it is stressed that during the DNMR experiment the samples are in the dark. Thus the initially present *cis*-isomers convert into the *trans* state as a function of time. Consequently, if there is any correlation between the concentration of *cis*-isomers and the molecular orientational order, the DNMR line splittings that contain such order information should also exhibit time dependence. Indeed, the DNMR spectra of 7AB(D) and 8CB:7AB(D), as well as 8CB(D):7AB, exhibit such time-dependent changes. For example, in Figs. 4(a)–4(c) we show typical results obtained for 7AB(D), 8CB(D):7AB, and 8CB:7AB(D). These spectra were averaged for a period much shorter than the time scale of the observed changes; effectively, a ''snapshot'' view at each instant is so obtained. In addition to the *trans* doublet found in the *trans* samples, a second, inner doublet of smaller frequency splitting appears for the UV-illuminated 8CB:7AB(D) and 7AB(D) samples [Figs. 4(a)–4(b)]. Note that (i) the intensity (the area under the two associated absorption peaks) of the inner doublet decreases with time; also (ii) the intensity of the *trans* doublet increases by the same amount; (iii) the inner doublet is not present in the 8CB(D):7AB spectra, a sample lacking DNMR-sensitive 7AB(D) molecules. It then follows that such a time-dependent doublet belongs to *cis*-isomers. The disappearance of the *cis* peaks with time, reflecting the *cis*-to-*trans* thermal conversion, is also accompanied by a small increase in the *trans* and *cis* doublet frequency splittings $\Delta\nu_{trans}(t)$ and $\Delta\nu_{cis}(t)$, respectively. A similar increase in frequency splitting is found in $\Delta\nu_{8CB}(t)$ of the 8CB(D):7AB sample; this demonstrates that *cis*-isomerization-induced changes in the scalar order parameter of the 8CB(D) system are being detected.

The experimentally measured behavior is schematically shown in Fig. 5. The intensity I of a spectral doublet assigned to a certain molecular state, in our case the *trans* and *cis* states, is proportional to the number of molecules found in that state. The fraction c of *cis*-7AB molecules that are in *cis* form is determined from the relation

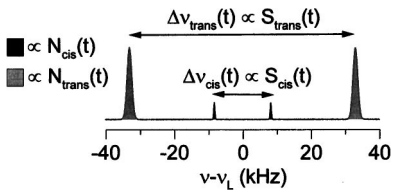

FIG. 5. Typical spectrum of a UV-illuminated 8CB:7AB(D). Peak intensities are proportional to the respective populations of *cis*-7AB and *trans*-8CB isomers. In the dark, populations and doublet frequency splittings exponentially approach with time the equilibrium value.

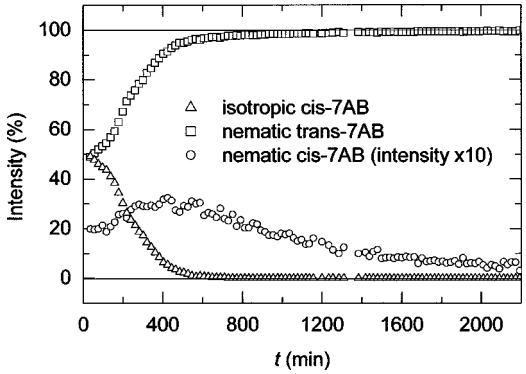

FIG. 6. Time dependence of the 7AB(D) DNMR spectrum doublet frequency splittings at $T=308.6$ K. The sample was exposed to UV light for about 180 min and then measured in the dark.

$$c_{cis}(t)=\frac{I_{cis}(t)}{I_{cis}(t)+I_{trans}(t)}. \tag{5}$$

An additional feature of the 7AB(D) spectra in Fig. 4(a) is the presence of the absorption peak centered at zero frequency; it is associated with the isotropic phase of *cis*-7AB molecules since these do not form an orientationally ordered phase. UV illumination of 7AB thus yields a coexistence of the isotropic *cis*-7AB phase and the nematic phase. The nematic phase is a mixture of *cis*-7AB (low-concentration) and *trans*-7AB (high-concentration) isomers, similar to what occurs in the 8CB:7AB mixture [see Figs. 4(b) and 4(c)]. The isotropic *cis*-7AB, the nematic *cis*-7AB, and the *trans*-7AB intensity contributions exhibit a time dependence that can be evaluated from the spectra in Fig. 4(a): see Fig. 6. From Fig. 6 is evident that the *cis* population in the isotropic phase decays significantly faster than the *cis* population in the nematic phase. The initial increase in nematic *cis* intensity demonstrates that upon conversion from the isotropic to the nematic phase, a fraction of the molecules retain their *cis* state. Further, the concentration of *cis*-7AB molecules in the nematic phase, calculated from Eq. (5) by neglecting the isotropic *cis* contribution to I_{cis}, exhibits a monotonic decrease in time that is visualized in Fig. 7(a). This is quite similar to the decay exhibited by the 8CB:7AB mixture seen in Fig. 7(b).

The experimentally determined time dependences of $c_{cis}(t)$ [Figs. 7(a) and 7(b)], $\Delta\nu_{trans}(t)$ [Figs. 8(a)–8(c)], and $\Delta\nu_{cis}(t)$ [Figs. 9(a) and 9(b)], calculated from the spectra presented in Figs. 4(a)–4(c), are consistent with an exponential time dependence. The respective characteristic times τ_c^{cis}, $\tau_{\Delta\nu}^{cis}$, $\tau_{\Delta\nu}^{trans}$, and $\tau_{\Delta\nu}^{8CB}$ can be calculated using the model functions

$$c_{cis}(t)=c_0\exp(-t/\tau_c^{cis}) \tag{6}$$

and

$$\Delta\nu_i(t)=\Delta\nu_\infty^i-\delta\Delta\nu_0^i\exp(-t/\tau_{\Delta\nu}^i), \tag{7}$$

with c_0 denoting the initial concentration of *cis*-7AB molecules with respect to the total population of 7AB molecules at $t=0$; clearly, c_0 is a measure of the effectiveness of the UV-illumination-induced photochemical isomerization. The subscript and superscript i in Eq. (7) refers to *trans*-7AB, *cis*-7AB, or 8CB depending on the molecule giving rise to the observed frequency splitting doublet $\Delta\nu_i(t)$. $\delta\Delta\nu_0^i$ is the initial change in the frequency splitting measured compared to $\Delta\nu_\infty^i$, which is the frequency splitting in the $t\to\infty$ limit. $\Delta\nu_\infty^{trans}$ and $\Delta\nu_\infty^{8CB}$ match the frequency splittings of the pure sample [Figs. 3(a) and 3(b)], whereas $\Delta\nu_\infty^{cis}$ is a

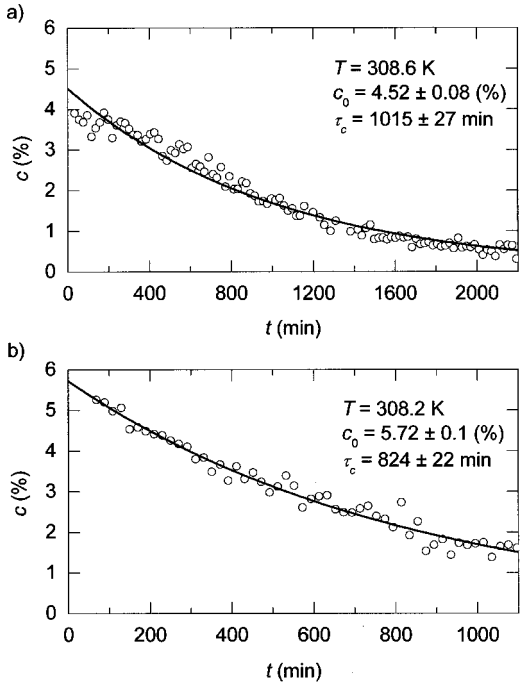

FIG. 7. Time decay of the *cis*-7AB isomer percent concentrations in (a) 7AB(D) and (b) 8CB:7AB(D) after removal of the UV exposure. Solid lines are exponential fits.

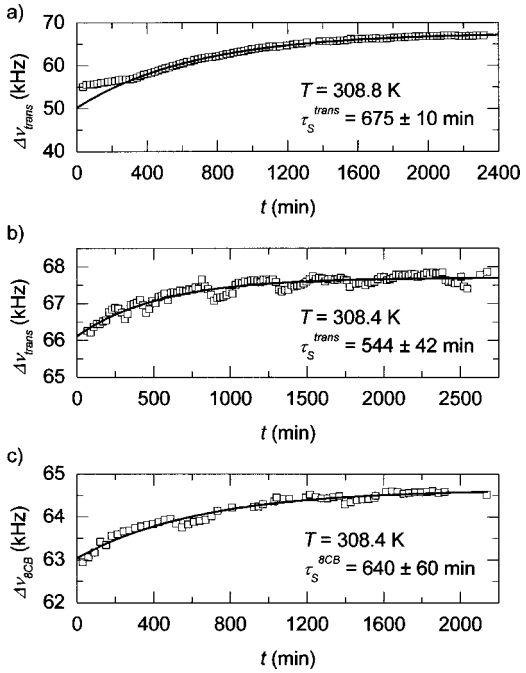

FIG. 8. Time dependence of the outer deuterium spectral doublet frequency splittings of (a) *trans*-7AB in 7AB(D), (b) *trans*-7AB in 8CB:7AB(D), and (c) 8CB in 8CB(D):7AB, after removal of UV illumination. The respective exponential fits are shown as solid lines.

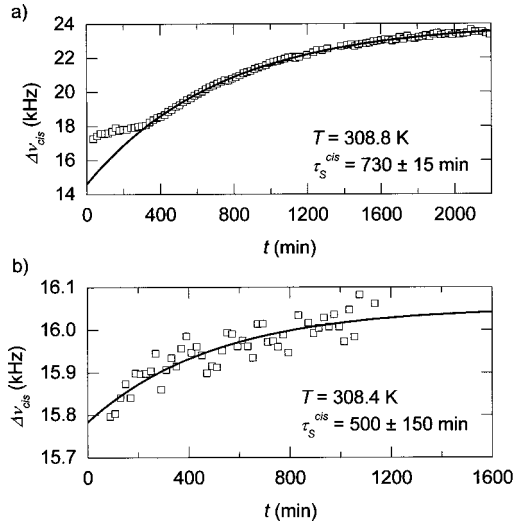

FIG. 9. Time dependence of the *cis*-7AB isomers deuterium doublet frequency splitting in (a) 7AB(D) and (b) 8CB:7AB(D) after removal of UV illumination.

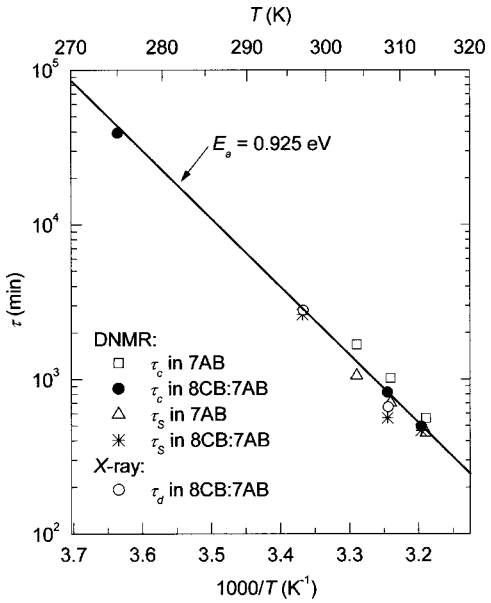

FIG. 10. Temperature dependence of the characteristic times τ_c, τ_S, and τ_d. When fitted individually to the Arrhenius law, the five data sets yield similar values for the activation energy; thus, only an effective theoretical fit (dashed line) is shown.

model parameter and cannot be measured since in the $t \to \infty$ limit the number of *cis*-7AB isomers would be negligible. Given the proportionality between the DNMR frequency splitting and the order parameter, Eq. (1), it is possible to express the relative change in the nematic order parameter as

$$\frac{\delta S_i}{S_\infty^i}(t) = \frac{\delta S_0^i}{S_\infty^i}\exp(-t/\tau_s^i), \quad -1 < \frac{\delta S_0^i}{S_\infty^i} = \frac{\delta \Delta \nu_0^i}{\Delta \nu_\infty^i} < 0, \quad (8)$$

where the $\Delta\nu$'s associated with the characteristic times were replaced with S's. This is done to stress that the observed time dependence of the frequency splitting implies a change in nematic order: i.e., τ_s measures the characteristic time to reestablish the nematic order S_∞^i of pure samples with zero *cis*-7AB population.

The DNMR study allows us to determine eight physical parameters relevant for the description of photoisomerization-induced structural changes in the investigated systems: c_0, τ_c, τ_S^{trans}, τ_S^{cis}, τ_S^{8CB}, $\delta S_0^{trans}/S_\infty^{trans}$, $\delta S_0^{cis}/S_\infty^{cis}$, and $\delta S_0^{8CB}/S_\infty^{8CB}$. They were measured at several representative temperatures in order to unveil possible correlations among them. The results are summarized in Table I. Values of c_0 obtained with steady UV-light illumination and values of the characteristic times for 7AB and 8CB:7AB are very similar at all temperatures. This confirms their primary dependence on temperature and on the internal molecular properties, whereas the molecular environment, i.e., the type of LC phase present, seems to only play a minor role.

The characteristic decay times, illustrated in Fig. 10, seem to conform to an Arrhenius law $\tau = \tau_0 \exp(E_a/kT)$ with activation energy $E_a = 0.925$ eV. Since the difference in τ_S^i values at a constant temperature is rather small, their averaged value was used to generate points shown in Fig. 10. Closer inspection reveals that the τ_c values at any temperature are systematically higher by 20–50% than the τ_S values. This is interesting as it means that the concentration of *cis*-isomers changes more slowly than the value of the scalar order parameter. Since we believe that the observed $\delta S(t)$ time dependence corresponds to an instantaneous adjustment of the nematic order due to changes in the *cis*-7AB concentration

TABLE I. Photoisomerization parameters determined from DNMR in 7AB(D), 8CB:7AB(D), and 8CB(D):7AB. Symbols: *N* is the nematic phase; Sm-*A* the smectic-*A* phase; c_0 is the initial concentration of *cis*-7AB molecules of the total population of 7AB molecules; τ_c represents the time decay of the *cis*-7AB isomer concentration; the τ_S's refer to the time decay of the respective outermost frequency splitting, i.e., to the characteristic time of the restoration of the orientational order to that of a non-UV-illuminated sample. The ratios in the last three columns refer to relative changes in the respective nematic order parameter.

T (K)	System	Phase	c_0 (%)	τ_c (min)	τ_S^{trans} (min)	τ_S^{cis} (min)	τ_S^{8CB} (min)	$\delta S_0^{trans}/S_\infty^{trans}$	$\delta S_0^{cis}/S_\infty^{cis}$	$\delta S_0^{8CB}/S_\infty^{8CB}$
313.6	7AB	*N*	3.84±0.13	560±30	430±15	465±20		0.33±0.015	0.47±0.04	
308.6		*N*	4.52±0.08	1015±27	675±10	730±15		0.25±0.015	0.38±0.02	
304		*N*	5.2±0.1	1670±70	1050±40	1055±65		0.20±0.02	0.29±0.02	
312.9	8CB:7AB	*N*	8.97±0.1	496±8	488±65	460±65	451±20	0.097±0.02	0.093±0.03	0.13±0.005
308.2		Sm-*A*	5.72±0.1	824±22	544±42	500±150	640±60	0.024±0.008	0.017±0.006	0.024±0.008
296.9		Sm-*A*					2620±240			0.005±0.002
275		Sm-*A*	4.6±0.5	39000±4000						

$c(t)$, τ_S is expected to more closely match τ_c. However, this expectation can only be valid if $\delta S(t)$ and $c(t)$ are linearly related. A power law dependence $\delta S(t) \propto c^{\kappa}(t)$, on the other hand, preserves the experimentally confirmed exponential nature of $\delta S(t)$ by simultaneously rescaling the characteristic time to $\tau_S = \tau_c / \kappa$. A $\kappa > 1$ can account for the observed discrepancy. This speculation suggests an equality between the activation energies for the $c(t)$ and $\delta S(t)$ processes. When E_a values are separately fitted to each of the four data sets shown in Fig. 10, they are in very good agreement, with κ accounting for the differences in τ_0 values.

C. Origin of the photomechanical effect in 8CB:7AB

Comparing the above DNMR results on characteristic relaxation times with the typical times for layer thickness changes (Fig. 10, open circles) obtained from small-angle x-ray scattering measurements [14], one sees a remarkable agreement. In other words, the decrease in nematic order $\delta S(t)$ and the increase in layer spacing $\delta d(t)$ both reflect the presence of the *cis*-7AB isomers, $c(t)$. The photoinduced changes in the layer thickness can be explained by considering the relation between the orientational order of the molecules within the layers and the layer thickness. In smectic-*A* phases of rodlike molecules possessing two aliphatic chains, one at each end of an aromatic core, the layer thickness *d* and the nematic order parameter *S both decrease* with increasing *T* [29]. In contrast, in 8CB, smectic layers consist of dimers [30] and, while *S decreases, d increases* with *increasing T* [14]. The same qualitative behavior is found in the 8CB:7AB mixture [13]. DNMR data on this mixture [Fig. 3(b)] show that *S decreases* with *T*; consequently, *S* (equivalently, $\Delta\nu$) *decreases with increasing d*. The relation $\Delta\nu(d) \propto S(d)$, calculated by combining $d(T)$ data from [14] with the $\Delta\nu(T)$ data of Fig. 3(b), shows an almost perfect linear dependence, which is presented in Fig. 11. In a naive scenario it can be assumed that the orientational order parameter and the layer thickness are directly correlated, i.e., a decrease in *S* yields a linear increase in *d*, and that such an *S-d* interplay is the prevailing mechanism responsible for the variation of *d*. The photomechanical effect observed in the 8CB:7AB sample can therefore be described in terms of UV-illumination-induced changes in *S*, resulting in changes in *d* through the *S-d* interplay. The actual situation seems to be subtler, as discussed below.

Given the above interpretation, UV illumination at constant *T* is equivalent to an increase in *T* in the darkness; both sample treatments should drive the system along the *S-d* or, equivalently, the $\Delta\nu$-*d* curve of Fig. 11. Let us consider the behavior at two representative temperatures $T_{\mathrm{low}} = 297$ K and $T_{\mathrm{high}} = 308.3$ K. The states of the system in the *S-d* diagram are denoted with A_{low}, B_{low}, B'_{low} and A_{high}, B_{high}, B'_{high}, respectively. There, the *A* state represents the condition of a pure, non-UV-illuminated sample. The $A \rightarrow B$ path is achieved by isothermal UV treatment (wavy lines in Fig. 11). The relative shift of the *B* state with respect to *A*, denoted by $(\delta d, \delta\Delta\nu)$, was experimentally determined from the x-ray scattering results for $d(T)$ from [14] and the $\Delta\nu(T)$ data seen in Fig. 3. If the increase in *d* was only due to the *S-d* interplay, the respective final state B' would be located along the *S-d* curve of the pure sample, which is represented by

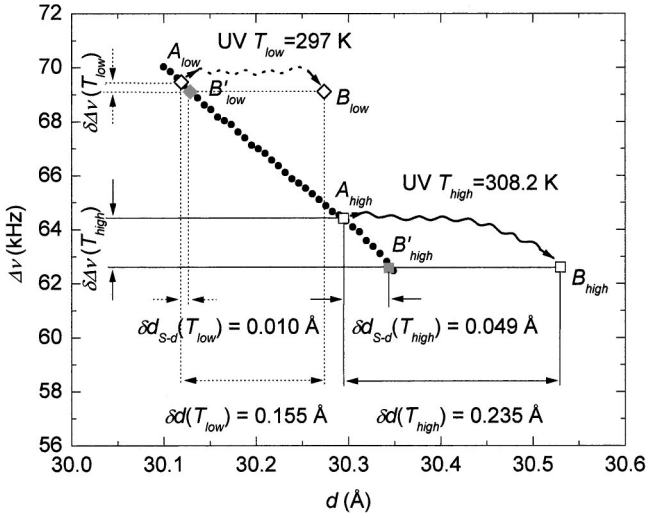

FIG. 11. Deuterium doublet frequency splitting vs layer thickness in 8CB:7AB(D) (solid circles). The effect of UV illumination, sketched at the two temperatures T_{low} and T_{high}, can be regarded as an isothermal transition from point *A* to point *B*, yielding a layer thickness increase of δd. The direct orientational order-parameter–layer-thickness interplay (*S-d*), which would shift the state along the quasilinear $\Delta\nu$-*d* curve (defined by the solid circles) by a small amount $\delta d_{S\text{-}d}$, does not account for the measured increase in δd.

solid circles in Fig. 11, with relative coordinates $(\delta d_{S\text{-}d}, \delta\Delta\nu)$ with respect to *A*. This is not the case since one observes $\delta d_{S\text{-}d} \ll \delta d$ at both T_{low} and T_{high}. Therefore, the experimentally observed photomechanical effect exceeds considerably what would be expected from an *S-d* interplay. It is thus reasonable to conclude that some kind of structural rearrangement takes place in order to account for the relatively large change in the layer thickness.

The DNMR results here described provide indirect support for a nanophase segregation picture where the *cis*-7AB molecules are driven to locations between the layers. This is specifically suggested by the estimate [16,21] that only about 5–7 % of the 7AB molecules may be converted to the *cis* state in order to quantitatively satisfy the experimentally determined increase in *d* with UV illumination. In fact, the initial concentrations c_0 of the 7AB isomers, as determined in our study and summarized in Table I, are in excellent agreement with such an estimate. Yet a remaining question that now arises is whether only a fraction of the *cis*-7AB isomers are squeezed out from the smectic layers. If this were the case, the presence of isomers embedded in the layers and those segregated in the interlayer spacing would result in two spectral doublets of distinct frequency splitting. This, however, is not the type of DNMR spectral pattern observed [Fig. 4(b)]. Consequently, the existence of a single spectral doublet (apart from the *trans*-7AB doublet) arising from the *cis*-7AB isomers suggests that practically all isomers undergo phase segregation.

D. Effective local symmetry of *cis*-7AB

The sharpness of the resonance lines in Fig. 4(b) proves that all *trans*-7AB isomers ''see'' the same physical environment. The same holds for the *cis*-7AB isomers. Unlike *trans*-7AB, the *cis* molecules are highly bent and the two alkyl chains on either side of the molecular core could give rise to

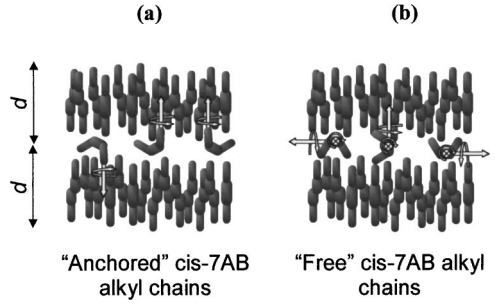

FIG. 12. Two possible configurations of the nanosegregated *cis*-7AB isomers in the interlayer region. The two alkyl chains are physically nonequivalent in ''anchoring'' arrangement, giving rise to two distinct *cis*-7AB DNMR doublets. Since only one doublet has been detected, the ''free'' configuration is more probable.

different DNMR frequency splittings. This might occur, for instance, if the first of the alkyl chains was anchored to the layer and aligned along the layer's normal, while the second alkyl chain is rotated around the long axis of the anchored chain, as depicted in Fig. 12(a). The two deuterons in the anchored chain would contribute a spectral doublet $\Delta\nu_{cis}$ of magnitude near that of $\Delta\nu_{trans}$ (or, equivalently, $S_{cis}\approx S_{trans}$), which may not be distinguishable from the *trans* splitting doublet. Further, from Eqs. (2)–(4) with $\vartheta_1=0°$ and $\vartheta_2=\phi_0=62°$, $\Delta\nu_{cis}$ from the deuterons in the reorienting alkyl chain, at any orientation and temperature, would be smaller by a factor of $\Delta\nu_{cis}/\Delta\nu_{trans}=S_{cis}/S_{trans}=P_2(\cos\phi_0)\approx 0.16$.

To verify such predictions we studied in greater detail how the orientational order parameter $S\propto\Delta\nu$ depends on temperature in the 8CB:7AB(D) mixture: see Fig. 13(a). The ratio of *cis* to *trans* order parameters, S_{cis}/S_{trans}, calculated

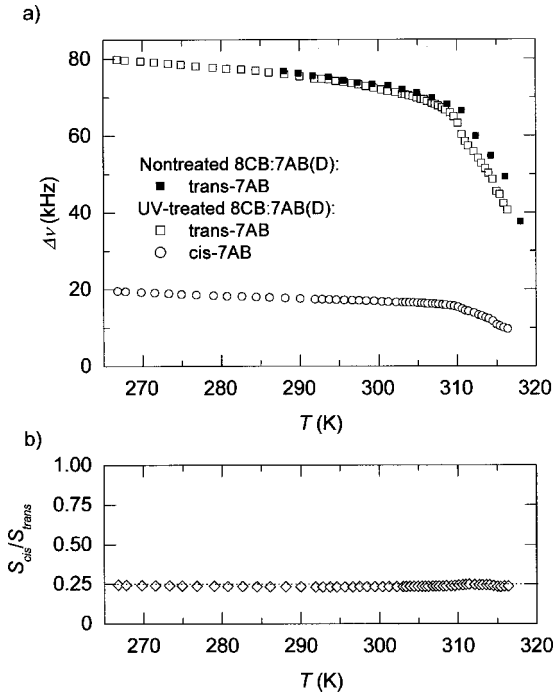

FIG. 13. (a) Temperature dependence of the DNMR frequency splitting in 8CB:7AB(D) and (b) the ratio of the *cis*-7AB and *trans*-7AB orientational order parameters in a UV-treated sample.

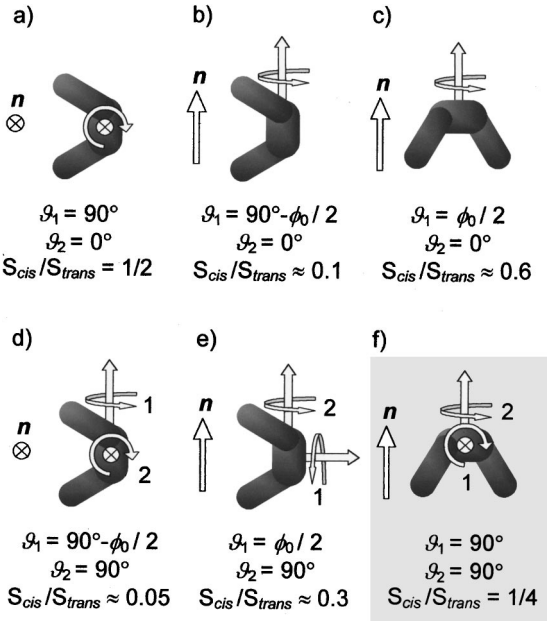

FIG. 14. Simple one-axis and two-axis reorientational modes of the *cis*-7AB molecule. **n** is the normal to the smectic layers. Mode (f) gives a S_{cis}/S_{trans} ratio that better matches the experimental value. $\phi_0\approx 62°$ is the effective angle between the two heptylazobenzene rodlike molecular fragments.

from the data in Fig. 13(a) and Eq. (4) is shown in Fig. 13(b). Within experimental accuracy, this ratio is independent of temperature with an average value$\approx$0.24. This is inconsistent with the previously discussed ''anchoring'' scenario of Fig. 12(a) where $S_{cis}/S_{trans}\approx 1$ and $S_{cis}/S_{trans}\approx 0.16$ corresponded to the anchored and the free rotating alkyl chains, respectively. The appearance of a single spectral doublet caused by *cis*-isomerization of 7AB confirms the physical equivalence of the two alkyl chains. It may not be fortuitous that the experimental value of S_{cis}/S_{trans} is very close to 1/4, since such rational numbers are expected for some typical reorientational dynamics modes for bent molecules. Their effect on the orientational order parameter, and consequently on the DNMR doublet frequency splitting, was qualitatively discussed in Sec. III A.

The basic reorientational one-axis and two-axis modes are found in Fig. 14. Specifically, the two-axis reorientational motion of the type seen in Fig. 14(f), with $\vartheta_1=\vartheta_2=90°$, yields $S_{cis}/S_{trans}=1/4$. DNMR results thus support a model where the bent, boomerang-shaped *cis*-7AB molecules that are segregated from the smectic layers perform fast reorientations (characteristic time τ_1) about the axis perpendicular to the boomerang plane. With time, this axis quickly reorients (τ_2) in the plane of the adjacent smectic layers. The characteristic times τ_1 and τ_2 for the two types of reorientational motion are much shorter than the DNMR time scale $\tau_{\mathrm{NMR}}\approx 2\times 10^{-5}$ s (Sec. III A) due to the sharpness of the *cis*-7AB(D) resonance lines, reflecting complete motional narrowing. On the other hand, τ_1 and τ_2 are expected to be longer than the reorientational time $\tau_{\mathrm{rot}}\approx 2\times 10^{-9}$ s for an elongated 8CB molecule about its long axis [31].

The above dynamics implies a uniaxial effective local symmetry of the *cis*-7AB isomers, and measurements of the angular dependence of the spectral doublets prove this. The

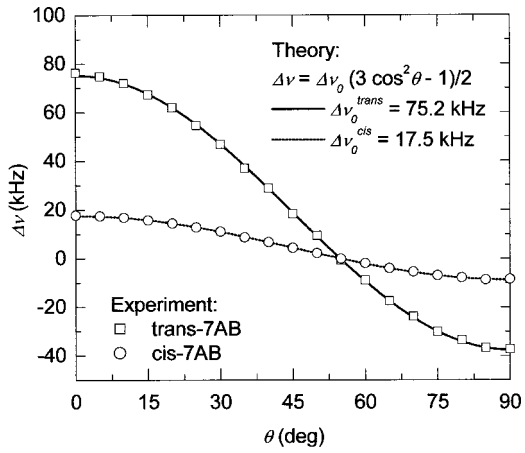

FIG. 15. Angular dependence of the DNMR *cis*-7AB and *trans*-7AB doublet frequency splittings in 8CB:7AB(D) which is reminiscent of uniaxial local symmetry.

frequency splitting angular dependence obtained at $T = 291\,\mathrm{K}$ is shown in Fig. 15. $\Delta\nu(\theta)$ for both *trans*-7AB and *cis*-7AB follow the typical $P_2(\cos\theta)$ dependence, reminiscent of uniaxial symmetry. The relatively low temperature was chosen and the angular pattern total measurement time kept below 300 s in order to preserve the layered structure while reorienting the sample in the field. At higher temperatures or for longer measurement times, the layered structure is destroyed since the director tends to orient parallel to the external magnetic field; equivalently, smectic layers tend to be oriented perpendicularly to B_0.

V. CONCLUSIONS

We have studied photoinduced changes in the molecular orientational order of the liquid crystalline mixture 8CB:7AB. In agreement with previous studies, the smectic-*A* phase of this mixture undergoes substantial changes in layer spacing under UV (expanding) or visible (contracting) light irradiation [12–14,21]. Previous studies also revealed that the increase in layer spacing is related to a *trans*-to-*cis* isomerization of the 7AB molecules upon UV illumination, while the decrease in layer spacing is related to the relaxation of the *cis*-isomers into the ground *trans* state. Moreover, computer simulations [16] showed the possibility of nanophase segregation in which the photoinduced *cis*-7AB isomers change their positional order and move from within the layers to locations between the layers. What was unknown is the behavior of the orientational order parameter of the liquid crystal undergoing all these photoinduced transformations.

The present study shows that DNMR is an extremely powerful technique to characterize structural changes including their dynamics in photosensitive liquid crystals. Our study reveals that upon UV illumination, only a small fraction of the *trans*-7AB isomers is converted into *cis*-isomers. A reduction of the overall orientational order of the system, whether pure 7AB or the 8CB:7AB mixture, is found whenever *cis*-isomers are present. The 7AB *cis*-isomers are unambiguously identified in the DNMR spectra through the appearance of an additional absorption frequency doublet. In addition, the DNMR spectra indicate that the 7AB *cis*-isomer population decreases exponentially once the UV irradiation is turned off. Simultaneously, the orientational order parameter exponentially increases to the value characteristic of a pure, nonirradiated sample. This reflects an adjustment of the order to the changing fraction of 7AB *cis*-isomers; these isomers act as a disorienting factor that decreases the orientational order of the smectic-*A* phase.

A comparison of DNMR and x-ray studies [14] shows that the orientational order parameter and the layer spacing in pure 8CB and the 8CB:7AB mixture are related even without photoisomerization (or, equivalently, in the dark). The smaller the scalar order parameter *S*, the larger the layer separation *d*. When combined with the disorienting action of the 7AB *cis*-isomers, the *S*-*d* interplay model suggests that the photoinduced changes of the layer spacing *d* are a consequence of changes in *S*. For instance, UV irradiation increases the fraction of 7AB *cis*-isomers; this decreases *S* and consequently increases *d*. Although such a *S*-*d* interplay model is certainly valid, it does not yield a straightforward interpretation for the complete set of results. Specifically, the photoinduced changes in layer spacing *d* measured by x-ray scattering are too large to be fully accounted for by the *S*-*d* model. We thus conclude that nanophase segregation of 7AB *cis*-isomers must occur such that most of them migrate to locations between the smectic-*A* layers. A quantitative analysis of the effective volume of such a layer predicts a *cis*-isomerization of only a few percent; the DNMR data confirm that the isomerization effectiveness in the 8CB:7AB system is low.

Finally, this study supports a scenario where the bent, boomerang-shaped *cis*-7AB molecules segregate out of the smectic layers and perform fast reorientations on the DNMR time scale in the interlayer space. These reorientations are about two independent axes giving rise to a uniaxial symmetry. Despite their nonmesogenic behavior in pure 7AB(D), the nanophase-segregated 7AB *cis*-isomers have uniaxial orientational order controlled by adjacent smectic layers.

ACKNOWLEDGMENTS

This work was supported by the NSF-STC ALCOM Grant No. 89-20147. We are particularly grateful to Mary Neubert and co-workers for providing us with the deuterated materials. B.Z. acknowledges the support and hospitality of the Department of Physics and the Liquid Crystal Institute at Kent State University where the measurements were performed.

[1] W. M. Gibbons, B. P. McGinnis, P. J. Shannon, and S.-T. Sun, Proc. SPIE **3635**, 32 (1999).
[2] I. Janossy, J. Nonlinear Opt. Phys. Mater. **8**, 361 (1999).
[3] F. Simoni and O. Francescangeli, J. Phys.: Condens. Matter **11**, R439 (1999).
[4] K. Ichimura, Supramol. Sci. **3**, 67 (1996).
[5] T. Marusii and Yu. Reznikov, Mol. Mater. **3**, 161 (1993).
[6] K. Ogura, H. Hirabayashi, A. Uejima, and K. Nakamura, Jpn.

J. Appl. Phys., Part 1 **21**, 969 (1982).
[7] T. Ikeda, T. Sasaki, and K. Ichimura, Nature (London) **361**, 428 (1993).
[8] H. G. Walton, H. J. Coles, D. Guillon, and G. Poeti, Liq. Cryst. **17**, 333 (1994).
[9] A. S. Zolot'ko and V. F. Kitaeva, Pis'ma Zh. Eksp. Teor. Fiz. **59** 34, (1994) [JETP Lett. **59**, 33 (1994)].
[10] M. V. Kozlovsky, V. P. Shibaev, A. I. Stakhanov, T. Weyrauch, and W. Haase, Liq. Cryst. **24**, 759 (1998).
[11] D. Nees and T. Wolff, Langmuir **12**, 4960 (1996).
[12] W. R. Folks, Yu. A. Reznikov, L. Chen, A. I. Khizhnyak, and O. D. Lavrentovich, Mol. Cryst. Liq. Cryst. Sci. Technol., Sect. A **261**, 259 (1995).
[13] R. W. Folks, Yu. A. Reznikov, S. N. Yarmolenko, and O. D. Lavrentovich, Mol. Cryst. Liq. Cryst. Sci. Technol., Sect. A **292**, 183 (1997).
[14] T. A. Krentzel, O. D. Lavrentovich, and S. Kumar, Mol. Cryst. Liq. Cryst. Sci. Technol., Sect. A **304**, 2341 (1997).
[15] Z. Sekkat, J. Wood, Y. Geerts, and W. Knoll, Langmuir **11**, 2856 (1995).
[16] Y. Lansac, M. A. Glaser, N. A. Clark, and O. D. Lavrentovich, Nature (London) **398**, 54 (1999).
[17] R. van Roij, P. Bolhius, B. Mulder, and D. Frenkel, Phys. Rev. E **52**, R1277 (1995).
[18] W. H. De Jeu and F. Leenhouts, J. Phys. (Paris) **39**, 869 (1978).
[19] S. Garg, K. A. Crandall, and A. Khan, Phys. Rev. E **48**, 1123 (1993).
[20] G. Zimmerman, L.-Y. Chow, and U.-J. Paik, J. Am. Chem. Soc. **80**, 3528 (1958).
[21] W. R. Folks, S. Keast, T. A. Krentzel, B. Zalar, H. Zeng, Yu. A. Reznikov, M. Neubert, S. Kumar, D. Finotello, and O. D. Lavrentovich, Mol. Cryst. Liq. Cryst. Sci. Technol., Sect. A **320**, 77 (1998).
[22] R. Y. Dong, *Nuclear Magnetic Resonance of Liquid Crystals* (Springer, New York, 1994).
[23] J. W. Doane, in *Magnetic Resonance of Phase Transitions*, edited by F. J. Owens, C. P. Poole, Jr., and H. A. Farach (Academic, New York, 1979).
[24] D. Catalano, C. Forte, C. A. Veracini, J. W. Emsley, and G. N. Shilstone, Liq. Cryst. **2**, 345 (1987); **2**, 357 (1987).
[25] J. W. Emsley, G. R. Luckhurst, and C. P. Stockley, Mol. Phys. **44**, 565 (1981).
[26] J. C. Rowell, W. D. Phillips, L. R. Melby, and M. Panar, J. Chem. Phys. **43**, 3442 (1965).
[27] P. G. de Gennes and J. Prost, *The Physics of Liquid Crystals* (Oxford University Press, Oxford, 1993).
[28] J. W. Doane, in *Nuclear Magnetic Resonance of Liquid Crystals*, edited by J. W. Emsley (Reidel, Dordrecht, 1985).
[29] A. De Vries, Mol. Cryst. Liq. Cryst. **16**, 311 (1972).
[30] P. E. Cladis, Mol. Cryst. Liq. Cryst. **165**, 85 (1988).
[31] J. Struppe and F. Noack, Liq. Cryst. **20**, 595 (1996).